Design of a High Aspect Ratio Wing Box using an Ant Colony Optimization Algorithm

Ricardo Diogo

ricardo.diogo@tecnico.ulisboa.pt

Instituto Superior Técnico, Universidade de Lisboa, Portugal

February 2016

Abstract

Every aircraft currently crossing the sky are using fossil fuels in order to generate the propulsion required to fly, which leads to the production of carbon dioxide and other greenhouse gases that warm the environment. Having this in mind, the main drive for the next generation of aircraft is fuel efficiency. One of the solutions that is being tested to increase the fuel efficiency is the introduction of high aspect ratio wings. A high aspect ratio wing leads to many structural problems, and to solve them one needs to have a considerably stiff wing box. The given solution increases the weight of the wing and reduces the advantages brought by the introduction of a high aspect ratio (AR) wing, thus making the design of the wing box a fundamental aspect. In order to have the stiffest possible structure having the minimum possible weight, one can do a topology optimization to find the optimal design for the given constraints. The main goal of this thesis is to find the optimal design of the wing box by performing a topology optimization using Ant Colony Optimization (ACO) algorithm. ACO is a meta-heuristic biologically influenced algorithm that has been proven to be useful to solve NP-hard combinatorial optimization problems in an expedite way. Its application to solve topology optimization has been introduced recently. Conclusions on the close to optimal topology of a wing box from a high aspect ratio wing are presented. In this thesis, a MATLAB$^{\circledR}$ code integrated with ANSYS$^{\circledR}$ for the structural analysis, is developed, in order to do a topology optimization. One will start by solving a literature case. Afterwards, the wing box of the NOVEMOR project of the EU 7th framework wing was optimized.

Keywords: ACO algorithm, Stochastic Search Method, Structural Topology Optimization, High Aspect Ratio Wings.

1. Introduction

In every action that one takes, one tries to find the optimal way to do it, from the quickest route to work, in order to avoid traffic, to a given mathematical application in which one is trying to find an optimum of a function. This concept is extremely important in our life, mainly due to every resource being finite, limited in some sort of sense.

The increase in number of flights, resulting from an ever increasing demand, has led to an estimate of 2.3 billion passengers and 38 million tonnes of freight on scheduled services, making a total of 531 billion tonne kilometre crossed by aircraft in 2010. These numbers are also translated in the economic impact that aviation has, generating roughly €220 billion and providing 4.5 million jobs [1]. It is expected that the number of passengers will increase at rate of 4.8% per year through the years until 2036 [2]. However, due to the restrictions imposed in CO_2 emissions, and other greenhouse gases and knowing that liquid fuels availability is finite, the development of the new generation of aircraft has as the main drive fuel efficiency and how one can one decrease the harm done by aviation to the environment.

One of the trends in aircraft development in order to increase fuel efficiency is the introduction of high Aspect Ratio (AR) wings. The introduction of a high AR wing it is not always easy to accomplish, leading to some problems, such as, structural, aeroelastic and control related ones.

Bearing this in mind, this thesis has as the main goal the implementation of a Topology Optimization using Ant Colony Optimization (ACO) algorithm to optimize a high AR wing. The ACO algorithm will be introduced along with the Topology Optimization with the most common approaches to solve this problem. The implementation of a Topology Optimization using the ACO algorithm and a literature case will be conducted. A high AR wing will be modelled, retrieving the aerodynamic loads for the given flight condition to apply to the struc-

tural model. Ultimately, the wing box will be optimized, being firstly the cross-section and afterwards a 3D optimization performed.

2. Background

Before performing the implementation of a Topology Optimization using ACO algorithm, a review of the given algorithm along side with the Topology Optimization was made.

2.1. Ant Colony Optimization algorithm

In recent years a lot of metaheuristic search techniques have been developed, being some of them nature-inspired algorithm, for instance, Genetic Algorithm, Simulated Annealing and Flower pollination. This trend of developing algorithms which try to recreate the natural processes is mainly due to the assumption that these processes are optimal, being this optimal state reached with a evolutionary process. This claim is hard to prove, because there are a lot of constraints in nature, from limited resources to the competition between all the species.

From these nature-inspired algorithms that have been developed in the recent years, one of the approaches used to solve the problems was to use the social behaviour of animal, such as insects, recreating the way they interact. This approach to problem solving is called Swarm Intelligence [3].

Ant Colony Optimization (ACO) is an algorithm that is inspired in the foraging behaviour of ants. Ants, when exploring the surrounding in order to find food, leave behind a trail of pheromone on the ground in order to mark the most favourable path for the other ants to follow. Ant Colony Optimization is inspired in this mechanism used by ants.

Marco Dorigo and colleagues in 1991 developed the ACO as a novel nature-inspired metaheuristic algorithm to solve hard combinatorial optimization problems (NP hard problems). From the initial work that Dorigo developed, many different variants from this algorithm were developed, such as, $MAX - MIN$ Ant System, Elitist Ant System, Rank-based Ant System. The one that will be described in this section is the Ant System [4], being the first ACO algorithm developed. The problem used to describe the implementation will be the Travelling Salesman Problem [5].

The combinatorial problems which the ACO can be applied to are in following form:

- $\mathbf{S}$, search space, being discretized over a finite decision variables X_i, $i = 1, ..., n$;

- X_i takes values in $D_i = v_i^1, ..., v_i^{|D_i|}$

- Ω, set of constraints for the variables

- f, objective function, $f : \mathbf{S} \to \mathbb{R}_0^+$

- s is a feasible solution if the assignment of values to all variables satisfies the constraints. s^* is a global optimum if and only if: $f(s^*) \leq f(s) \, \forall \, s \in \mathbf{S}$

In order to solve the Travelling Salesman Problem (TSP) one will simulate n_a (dimension of the colony) ants moving around the graph. Each ant is an agent which has the following characteristics [6]:

- able to choose one city at a time in order to find a solution. Each city will be chosen according to a probability, being this probability function of the town distance and the amount of pheromones in the edge that connects the towns;

- in order to have a Hamiltonian tour the towns that have been already visited cannot be visited again (tabu list);

- when a tour is completed, the agent will deposit pheromones in the edges (i, j) of its path accordingly to the pheromone update rule.

The steps that the algorithm will perform to find the optimal solution are described in Algorithm 1, which corresponds to the Ant System ACO [4].

Algorithm 1 Ant System ACO

1: **Initialize AS**

- Generate, $n_a = colony \ dimension$, ants

- Distribute randomly ants across the towns;

- Assign an initial value of pheromones, τ_{ij}, in the edges;

2: **for** $n = 1, ..., N$; $N = number \ of \ cycles$ **do**
3:     **for** $k = 1, ..., n_a$ **do**
4:         **while** Not Hamiltonian tour **do**
5:             Choose next town, using the *Transition Probability Rule*
6:         **end while**
7:     **end for**
8:     Distribute the pheromone, τ_{ij}, across the edges;
9: **end for**

2.2. Topology Optimization

Topology Optimization (TO) tries to find where one should place material in order to have the optimum topology for the given problem. The problem of finding the optimum configuration and spatial sequence of members and joints of a skeletal structure also belongs to the given optimization problem.

Bendsøe and Kikuchi [7] developed the first finite element based topology optimization for higher volume fraction, where the Homogenization approach

to solve the topology optimization problem was introduced. Almost at the same time, the SIMP approach was developed by Bendsøe [8]

The given problem of shape topology is transformed into a material distribution problem using a composite material. The composite material is constituted by substance and void, being the optimal microscopic void distribution the problem solved. This approach "is applied to determine macroscopic constitutive equations for the material with microscopic material distribution" [7].

The topology problem can be transformed into a sizing problem with the introduction of a material function density distribution in which one considers a composite consisting of an infinite number of small holes periodically distributed, being the on-off nature of the problem in a microscopic scale and not in the macroscopic one.

One will start by choosing the design domain and the finite element discretization that wants to use, consisting each element of a cellular material with a specific microstructure. The microstructure chosen should allow the density of the material to cover the whole range of values, from 0 (void) to 1 (solid). One option for a microstructure is a square cell with a centred rectangular hole. The square cell with a rectangular hole microstructure can be seen in Figure 1.
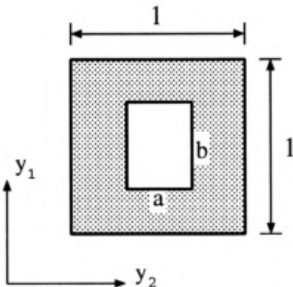

Figure 1: Unit cell with rectangular centered hole [9].

One of the approaches introduced after the Homogenization approach was the SIMP or power-law approach, where one uses Solid Isotropic Microstructures with Penalization for intermediate densities. SIMP was introduced by Bendsøe [8], with the goal of removing the discrete nature of the topology optimization by introducing the density variable, a continuous variable.

SIMP uses a pseudo-density as a design variable, being the relation between the density variable and the effective material stiffness given by the power law,

$$E(\rho_i) = g(\rho_i)E_0, \qquad (1)$$

where ρ_i is the density of the element i, E_0 is the Young's Modulus of the material and g is a penalization function, responsible to make the density variable tend towards 0 or 1. The penalization function proposed by Bendsøe [8] is represented by

$$g(\rho_i) = \rho_i^p, \qquad (2)$$

where p represents the penalization parameter. When $p = 1$, for the compliance objective function, the problem solved is a convex problem with a unique solution.

3. Topology Optimization using ACO

Ant Colony Optimization being a metaheuristic algorithm displays some advantages when solving a TO problem. One of the advantages that ACO presents when compared to a gradient-based algorithm is that it allows the use of a wider variety of objective functions. With a metaheuristic algorithm one just needs a function that describes the performance of the solution, using a gradient-based algorithm one needs a differentiable objective functions, due to the search process being based on the gradient of the objective function. In a metaheuristic algorithm the search process will be done using a stochastic process.

In order to use the ACO Ant System to perform Topology Optimization, one needs to do some changes to the original algorithm. The implementation of a topology optimization of a 2D beam subjected to a point load in its extremity and constrained in two points will be used as benchmark of the developed code. The implementation of the ACO in a TO problem will be done using the work of Kaveh and colleagues [10] as a reference.

The optimization problem that one will solve can be stated as

minimize: $U(\overline{\boldsymbol{u}})$

subject to: $\dfrac{V_f(\overline{\boldsymbol{u}})}{\overline{V_f}} \leq 1$, and physical constraints,

where $\overline{\boldsymbol{u}}$ represents the field displacement, $V_f(\overline{\boldsymbol{u}})$ corresponds to the volume fraction of the given solution, and $\overline{V_f}$ is the maximum volume fraction allowed. The physical constraints require that the element where the load is applied and the support elements must be present in the final design, and that the structure must be a connected structure, meaning that one must be able to find a continuous path that connects all the elements with the physical constraints.

In the current work, the objective function selected to optimize the structure will be the strain energy, which one wants to minimize. One needs to discretize the objective function, to have its representation across the discrete domain. The objective

function discretized across the domain is given by

$$U(\overline{\boldsymbol{u}}) = \frac{1}{2} \sum_{e=1}^{N} \int_{V^e} \varepsilon^T(\overline{\boldsymbol{u}}) D^e \varepsilon(\overline{\boldsymbol{u}}) dV, \qquad (3)$$

where V_e is the volume of the element in the domain, where the integral represents the strain energy of which, being the total strain energy of the domain equal to the sum of the strain energies from which element (N). ε represents the strains and D^e is the constitutive matrix of the element.
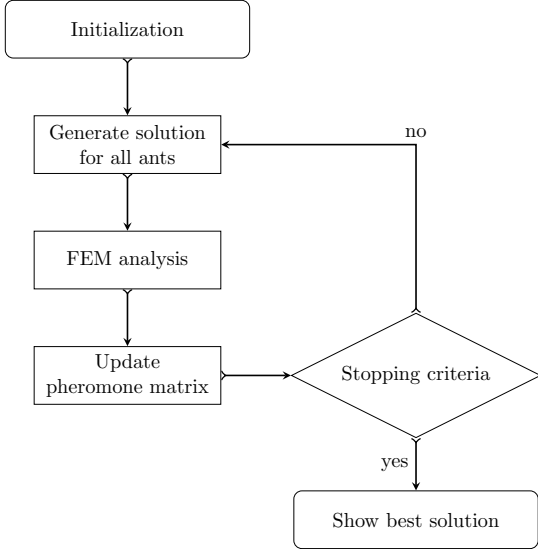
Figure 2: Flowchart for ACO applied for a topology optimization.

The optimization process for ACO applied for a TO is described in Figure 2.

In the given implementation the solution search will end when the given solutions have achieved the maximum volume fraction defined and the boundary conditions are met. One imposes the solution search until the maximum volume fraction has been reached, in fact the minimum strain energy will be found for the full design domain. So, the given problems that one has to solve is the distribution of that amount of material.

3.1. Element Transition Rule

Instead of having a Transition Probability, one will have an Element Transition rule. The Element Transition rule corresponds to the probability that a given element has to be selected as the next move for an ant, being given by [10]

$$P_i = \frac{(\tau_i(t))^\alpha}{\sum_{j=1}^{N} (\tau_j(t))^\alpha}. \qquad (4)$$

The probability of an ant choosing the element i is equal to the intensity of pheromone trail present in the element i to the power α, dividing by the sum of the intensity of pheromone trail to the power α of all the elements which are valid to as a next step. $\tau_i(t)$ represents the pheromone trail in element i in the t iteration of the optimization process. The parameter α is used to control the relative weight of the pheromone trail, one should be careful when doing the tuning of this parameter, because it can lead to premature convergence to non-optimal solutions.

3.2. Pheromone Update

The pheromone intensity $(\Delta \tau_i^k)$ laid by ant k in the element i, will be given by

$$\Delta \tau_i^k = \frac{(U_i^k)^\lambda}{\sum_{j=1}^{N} (U_j^k)^\lambda}, \qquad (5)$$

where U_i^k is the strain energy of element i of the solution obtained by ant k, λ is a parameter used to tune the influence of the strain energy in the algorithm, helping with its convergence.

After having the increment in pheromones for every element from all the solutions found by the ants, one can do the update of the Pheromone Matrix. The update of the pheromone matrix will be updated accordingly to the Pheromone Update Rule [11],

$$\tau_{ij}(t+n) = \rho \cdot \tau_{ij}(t) + \sum_{k=1}^{n_a} \Delta \tau_{ij}, \qquad (6)$$

where ρ is the evaporation rate and n_a is the dimension of the colony.

3.3. Noise Cleaning Filter

In order to improve the results generated by ACO for a TO problem, a noise cleaning filter during the pheromone update was introduced [10] to prevent the formation of tiny members in the structures obtained.

The noise cleaning filter will change the strain energy of the element, modifying the strain energy of an element with the strain energy of the neighbour ones. The modified strain energy will be given by

$$\hat{U}_i = \frac{\sum_{e=1}^{n^i} H_e U_e}{\sum_{e=1}^{n^i} H_e}, \qquad (7)$$

where H_e is the filter being given by

$$H_e = V_e \left[r_{min} - r(i,e) \right], \ e \in \left\{ 1, 2, ..., n^i \right\}, \qquad (8)$$

where V_e is the volume (or area in a 2D problem) of the element e, r_{min} is the minimum size allowed for the structure members, $r(i,e)$ is the distance between element i, which strain energy is being modified, and element e, a neighbour of element i that satisfies $r(i,e) \leq r_{min}$, n^i is the number of elements that satisfy the last condition.

3.4. Results

Having the code developed, one needs to solve a simple case in order to validate its performance and be sure that the outcome of the optimization is valid. In Kaveh et al.[10], two 2D problems were solved, being one of these cases selected to compare the output of the code developed. The one selected is the cantilever beam with a point load at its extremity. The modulus of elasticity (Young's modulus) and the Poisson's ratio used are equal to $7.9 \cdot 10^9 \ Pa$ and 0.30, respectively, being the same values used in Kaveh et al. [10].

Force [N]	10^4
Strain energy $[J]$	4.89
Max. Displacement $[m]$	$9.78 \cdot 10^{-4}$
Full Domain/Optimum [%]	65.44

Table 1: Strain energy for the optimum solution found in Kaveh et al. [10].

The strain energy of the full domain and the optimum solution found by Kaveh et al. [10] is shown in Table 1. Using the parameters summarized in Table 2, the cantilever beam problem was solved.

colony_dim	15
n_ite	30
evap (ρ)	0.3
alpha_p (α)	1
lambda (λ)	2.2
r_{min}	1.2

Table 2: ACO parameters used to obtain the best solution.
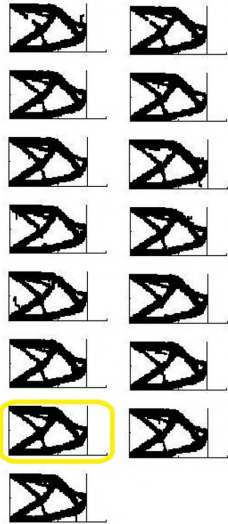
Figure 3: Solutins found at iteration 30

The parameters value were defined using the information obtained from the parametric study con-ducted.

The best solution, highlighted in Figure 3, displayed a strain energy equal to 4.875 J, matching the strain energy of the best solution found by Kaveh et. al. [10] (4.887 J). The solution displays some resemblances with the literature one, such as the overall shape and the central member which increases the stiffness of the structure. On the other hand, the solution obtained does not display symmetry as the one from the literature. The lack of symmetry is due to the random nature of the ACO metaheuristic algorithm.

4. High Aspect Ratio Wing Box Model

The wing used for the topology optimization problem that will be solved is based on the NOVEMOR project of the EU 7th framework reference wing. This wing was designed to present an high aspect ratio, $AR = 12$, while keeping the wing area, sweep, dihedral angle and the MTOW constants and equal to the reference wing [12].
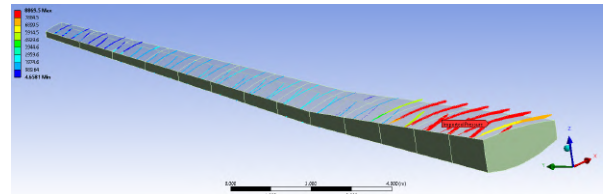
Planform Dimensions		
b	$[m]$	36.33
b_{r_b}	$[m]$	7.13
b_{b_t}	$[m]$	11.03
c_r	$[m]$	5.71
c_b	$[m]$	3.01
c_t	$[m]$	1.3
MAC	$[m]$	3.02
Λ	$[°]$	25
Γ	$[°]$	4.5

Table 3: Planform dimensions of the NOVEMOR 7th framework reference wing with $AR = 12$.
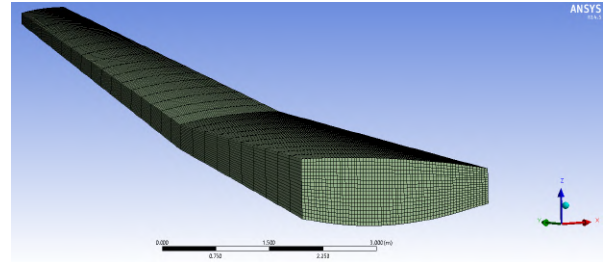
(a) ANSYS® mesh.

(b) Imported pressure from CFX® .

Figure 4: Wing box NOVEMOR 3D model.

Using the information from Table 3, one devel-

oped a 3D model in Solidworks® of the wing. During the development of the 3D model some simplifications were made when comparerd to the model used in Spada [12].

The whole wing was modelled in Solidworks® with the skin, ribs and a solid wing box, but to simplify the ANSYS® model, the only component used during the optimization process was the wing box, represented in Figure 4.

5. Cross-section 2D Optimization

One will start by the optimization of the wing box cross section. This problem will also correspond to a 2D optimization being the analysis of structure's performance conducted in 3D.

In order to optimize the wing box cross-section of the high aspect ratio wing, some modifications to the code were required.

Firstly, for the optimizer the problem solved will be two-dimensional, meaning that the optimizer will remain almost unaltered, requiring only the modification of the boundary conditions that the solutions need to satisfy. One has a pressure distribution, which will demand that all the elements of the upper and lower surfaces must be present in the solutions generated in order to be possible to perform a FEM analysis of the structure. The connectivity between the upper and lower surfaces must also be ensured, being this assured if the elements from the upper and lower surface are present in the solution.

Secondly, the structural problem solved is three-dimensional, having in mind that the optimization problem is 2D, one will need to relate the 3D structural elements with the 2D elements which represent the wing box cross-section. The "strain energy" ($u_{i_{2D}}$) of the 2D elements will be equal to the sum of the strain energy ($u_{ij_{3D}}$) of the set of 3D elements which are arranged longitudinally. The relation is given by

$$u_{i_{2D}} = \sum_{j=1}^{N_{long}} u_{ij_{3D}}, \qquad (9)$$

where N_{long} is the number of longitudinal divisions of the wing box ANSYS® model.

5.1. Results

The optimization of the wing box cross-section was performed using the model shown in section 4 and the value of the parameters with which one obtained the best solution for the literature case, given in Table 2. Two optimizations were performed, with a volume fraction (vol_f) equal to 0.35 and 0.45.

As seen in Figure 5, the solutions found at the end of the optimization process, a major part of the solutions display a connection between the upper and lower skin in both sides of the wing box.

One can also notice that the upper left and lower right corners of the wing box display a higher concentration of elements. The presence of the elements in these regions will increase the stiffness of the structure, when subjected to torsion. Being the angle of twist inversely proportional to the torsional constant of a Section, the torsional constant of a cross-section will increase if one has a higher concentration of material close to the boundaries of the cross-section.

The minimum strain energy obtained for vol_f equal to 0.35 and 0.45 at iteration 30, was equal to 14.783 J and 11.617 J, respectively. As expected, the solutions obtained at iteration 30 displayed a lower strain energy as the one obtained for a volume fraction equal to 0.35, being equal to 11.617 J. When comparing the results for both values of volume fraction, there is a relative decrease of 21.42 % when the volume fraction is increased from 0.35 to 0.45.
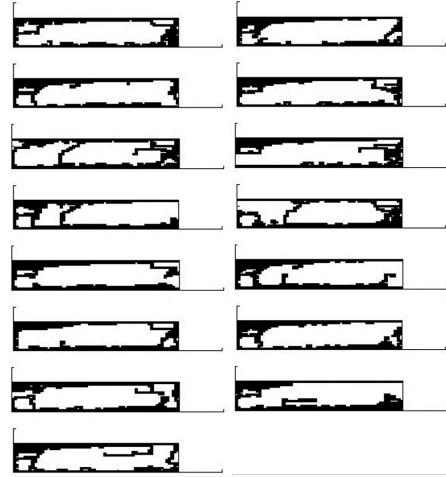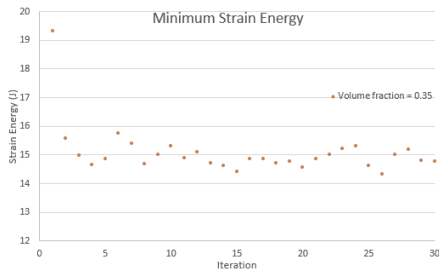

(a) vol_f = 0.35.
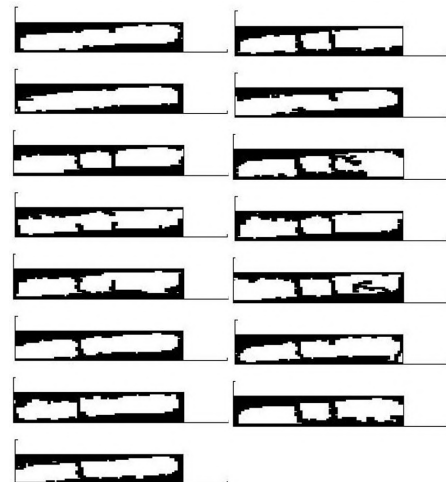
(b) vol_f = 0.45.

Figure 5: Wing box cross-section for iteration 30.

As seen in Figure 6(a), the minimum strain energy for `vol_f` equal to 0.35 after the first iterations displays a fluctuation around the value of 15 J, being the minimum strain energy equal to 14.783 J for the last iteration. The solution which displayed the minimum strain energy across the iterations displayed a strain energy equal to 14.329 J, being obtained at iteration number 26.

The maximum change in module of the strain energy will be equal to 0.696 J between iteration 26 and 27, corresponding to a relative change of 4.86 %. These small fluctuations can be explained with the stochastic behaviour of the algorithm and the small volume fraction used. During the solution generation, the ants will be placed in a random element of the domain in order to start the path's construction. Having a small volume fraction constrain, if the first element assigned does not belong to the optimum solution and is placed in a region which is not usual to have active elements the solution, some elements might be 'wasted' when trying to find the optimal solution, leading to the generation of a cross-section with a higher strain energy.

(a) `vol_f` = 0.35.
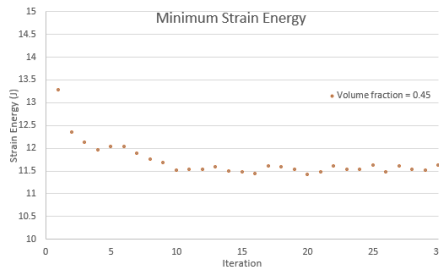
(b) `vol_f` = 0.45.

Figure 6: Minimum strain energy obtained throughout the optimization process.

With the increase of the volume fraction, `vol_f` equal to 0.45, one can notice also that the fluctuations of the minimum strain energy throughout the optimization process will have a lower magnitude, close to 0.1 J between iterations, as illustrated in Figure 6(b). This fact can be explained with the higher number of elements that the ants can select, meaning that the the absence of some elements from the solution will have a lower impact in the overall performance of the cross-section obtained.

To complete the optimization processes it was required 7 hours 11 minutes and 36 seconds for a volume fraction equal to 0.35 and 8 hours 11 minutes and 47 seconds for a volume fraction equal to 0.45, corresponding to 450 FEM analyses for each run, 15 per iteration for 30 iterations. The CPU used to perform the optimization was the Intel(R) Core(TM) i5-3350P CPU @ 3.10Ghz.

6. Full Span 3D Optimization

Having performed the optimization of the wing box cross-section using ACO, one extended the implementation in order to obtain the optimal 3D distribution of material for the wing box.

When compared with the cross-section optimization described in Section 5, the given optimization will have more freedom than if the topology optimization is restricted to the cross-section design.

The wing box structural model is composed of 29952 elements, corresponding to 1152 elements in the wing box cross-section, 18 in the y (vertical) direction and 64 in the x direction (chordwise direction), and 26 elements in the z direction (spanwise direction). If one used all the elements of the structural model as design variables, the computation time could increase drastically, so one decided to group elements, forming blocks with the structural elements using these blocks as design variables.

In the first instance, each block was formed by 4 elements in the z (vertical) and x (chordwise) direction and 1 element in the y (spanwise) direction, the given referential corresponds to the one used during the structural model generation, forming a 4 by 4 by 1 block composed of 16 elements of the structural mesh, represented in Figure 7. For the cross-section optimization, one gives emphasis to the cross-section discretization, meaning that the discretization of the cross-section would be finer than the mesh required for the FEM analyses. In order to have as much freedom as possible for the optimization having at the same time the minimum computation time possible, the resulting structural mesh had a finer discretization of the cross-section than in the longitudinal direction, therefore the blocks were constituted only by one element in the y direction.
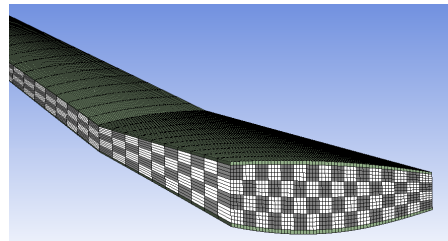

Figure 7: Structural mesh vs optimization mesh for blocks $4 \cdot 4 \cdot 1$.

For the last run, each block was formed by 2 elements in the z and x direction and 1 element in the y direction, resulting in a 2 by 2 by 1 block composed of 4 elements of the structural mesh.

The elements that compose the upper and lower surface of the wing box, in which the pressure distribution was applied, must be present. One decided that these elements would not be a part of the optimization process, being always present from the start in the solutions generation.

The connectivity between blocks during the optimization process will be identical to the one that one had during the 2D optimizations. Instead of demanding that the elements must share at least one edge, the corresponding of the edge in 3D would be the surface of the element. This demand resulted in a 6-elements neighbourhood during the element selection for the ant's path.

The resulting elements for each direction and for the structural mesh (st), $4 \cdot 4 \cdot 1$ blocks and $2 \cdot 2 \cdot 1$ blocks are given in Table 4.

	st	$4 \cdot 4 \cdot 1$	$2 \cdot 2 \cdot 1$
nelx	64	16	32
nely	18	4	8
nelz	26	26	26
nelem	29952	1664	6656

Table 4: Number of elements for each direction and different set of blocks.

6.1. Results

For the given problem, 3 runs were performed, two with 1664 and one with 6656 optimization blocks, referred as coarse and fine mesh, respectively. The two runs with the Coarse mesh were performed with a volume fraction vol_f equal to 0.35 and vol_f equal to 0.45, in order to compare with the results obtained for the cross-section optimization. The run with the fine mesh was performed with vol_f equal to 0.35.

The value of the ACO parameters used during the given runs will be equal to the ones used in the cross-section optimization, shown in Table 2.

6.1.1   Coarse Mesh

For vol_f equal to 0.35 the minimum strain energy obtained at iteration 30 was equal to 11.583 J, being the best solution represented in Figure 8, being equal to 9.830 J for vol_f equal to 0.45, represented in Figure 9 the best solution.

The strain energy obtained for vol_f equal to 0.45 is smaller than the one for vol_f equal to 0.35, as was expected.
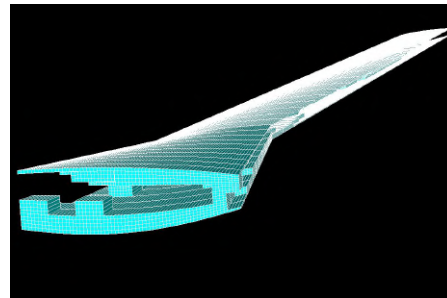
A higher concentration of elements can be seen close to the wing root, the elements concentration
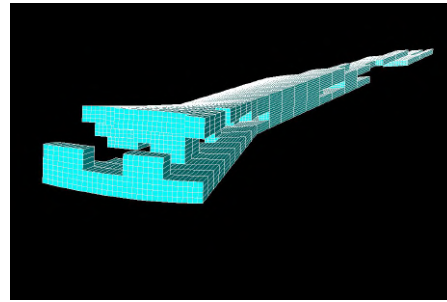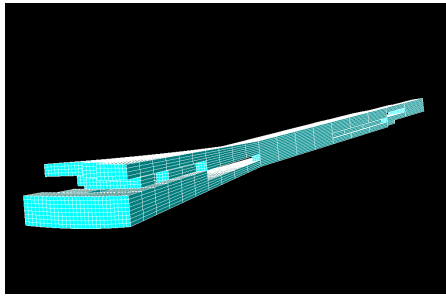

(a) Left half.
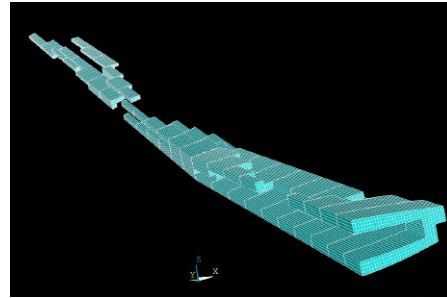
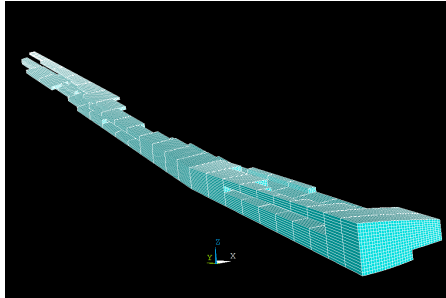(b) Right half.

(c) Wing box with skin.

Figure 8: Wing box cross solution vol_f = 0.35.

decreases in the spanwise direction. Close to the tip few elements are present, being connected to the rest of the structure by one member. As it can be seen in the pressure distribution across the surface of the wing box (Figure 4(b)), in the region close to the tip the magnitude of the pressure will be lower than the one close to the root, meaning that fewer elements will be necessary in that region to support the loads.

To complete the optimization processes it was required 7 hours 11 minutes and 36 seconds for a volume fraction equal to 0.35 and 8 hours 11 minutes and 47 seconds for a volume fraction equal to 0.45, corresponding to 450 FEM analyses for each run, 15 per iteration for 30 iterations, using the same machine where the cross-section 2D optimization was solved.

8

(a) Left half.

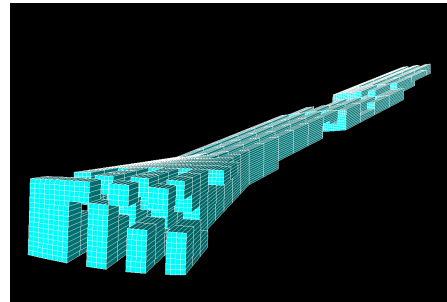(b) Right half.
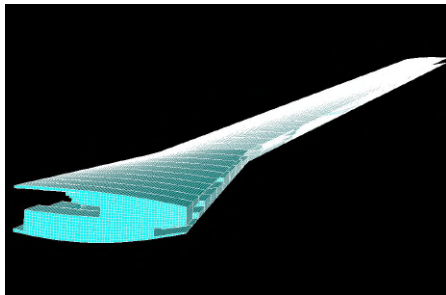
(c) Wing box with skin.

Figure 9: Wing box cross solution `vol_f` = 0.45.

(a) Left half.

(b) Right half.

(c) Wing box with skin.

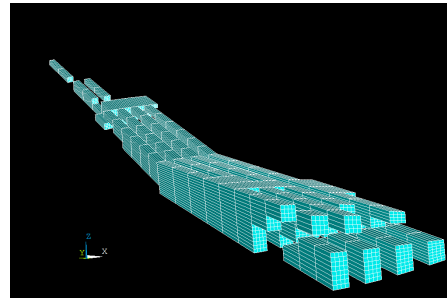Figure 10: Wing box solution for `vol_f` = 0.35.

6.1.2   Fine Mesh

Using $2 \cdot 2 \cdot 1$ blocks, one performed the given 3D optimization. The best solution at the end of the optimization process is represented in Figure 10. The strain energy of the given structure is equal to 11.129 J.

The solution obtained when compared with the one obtained for the $4 \cdot 4 \cdot 1$ blocks displays a different topology. One can notice lines of blocks along the spanwise direction, which will connect to each other at the middle of the wing. These lines of blocks can be seen close to the upper and lower surfaces of the wing box, being formed usually by two blocks side by side.
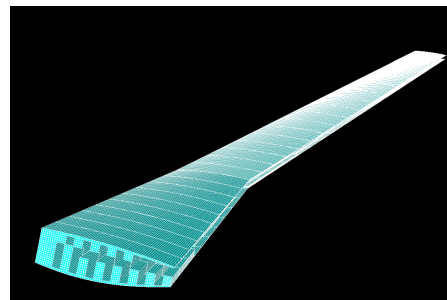
With the increase of blocks during the 3D optimization, one can notice a slight decrease in strain energy from 11.583 J for the coarse mesh to 11.129 J for the fine mesh. This decrease can be explained with the increase of freedom that the algorithm will have due to the increase of blocks available to se-

lect during the solution generation. Nonetheless, one should note that the given algorithm is meta-heuristic relying in a stochastic process to select the elements using at the same time some rules, meaning that for different runs with the same parameters, one can have different results.

To complete the optimization process it was required 102 hours 49 minutes and 54 seconds, corresponding to 450 FEM analyses, 15 per iteration for 30 iterations, using the same machine where the cross-section 2D optimization was solved.

6.2. 2D vs 3D Results

In Table 5, the values of strain energy for the cross-section and 3D optimization are shown, for the 3D optimization with `vol_f` equal to 0.35 the table entry displays the values for the coarse mesh and fine mesh, respectively. When the strain energy for the best solutions found in the cross-section and the 3D optimization is compared, one can notice that for both values of volume fraction one has a lower strain

9

energy value for the 3D optimization. Although, for both cases the volume fraction is the same, one will have more structural elements for the 3D optimization, because the elements that form the upper and lower skin of the wing box do not belong to the optimization problem, being always present. So for the same volume fraction, one always has more elements for the 3D optimization case. Nevertheless, the difference in strain energy is quite large and part of that difference may be due to the higher freedom in selecting the elements for the solution.

vol_f	0.35	0.45
Cross-section [J]	14.783	11.617
3D [J]	11.583/11.129	9.830
CPU time [s]	257439/370194	277070

Table 5: Minimum strain energy for the cross-section and 3D optimization.

From the cross-section optimization for the 2D optimization, one can also notice a drastic increase in the running time. This fact can be explained with the numbering of the elements. The structural elements are numbered in a crescent way in the span-wise direction, so one is performing the cross section optimization the elements which are removed from the matrices that the ANSYS® needs to solve will be sequential, taking less time to re-arrange the matrices. For the 3D optimization, the re-arrange of the matrices takes more time because the elements that need to be removed from the matrices are more dispersed.

7. Conclusions
The main objective of this work was to implement a topology optimization using the Ant Colony Optimization algorithm to perform a topology optimization of a high aspect ratio wing.

ACO has some advantages to implement in a topology optimization, such as its simplicity to apply to a discrete problem as the topology optimization, whereas most of the deterministic approaches usually require continuous design variables needing additional strategies to overcome this problem. Another advantage that the ACO brings is the flexibility to use any given objective function not being restricted to the differentiable ones.

On the other hand, ACO displays some drawbacks, making it not the most adequate algorithm to solve a topology optimization. Being a meta-heuristic algorithm requires that the performance of the solutions generated to be accessed at each iteration, which for the given problem, even having its complexity reduced, leads to high computational time. The increase of the number of design variable is also strictly related with the computation time.

In conclusion, ACO does not correspond to the most efficient algorithm to solve the minimum compliance problem (minimization of the strain energy).

References
[1] EU. Flightpath 2050 Europe's Vision for Aviation. Technical report, European Comission, 2011. Maintaining Global Leadership & Serving Society's Needs.

[2] ICAO. Aviation outlook, Environmental Report. Technical report, ICAO, 2010.

[3] James Kennedy and Russel C. Eberhart. *Swarm Intelligence*. Morgan Kaufmann Publishers, 2001.

[4] Marco Dorigo, Vittorio Maniezzo, and Alberto Colorni. Ant System: Optimization by a Colony of Cooperating Agents. *IEEE Transactions on Man, Machine and Cybernetics-Part B*, 26:29–41, 1996. February.

[5] David L. Applegate, Robert E. Bixby, and William J. Cook. *The Travelling Salesman Problem: A Computational Study*. Princeton University Press, 2006.

[6] Marco Dorigo and Thomas Stützle. *Ant Colony Optimization*. The MIT Press, 2004.

[7] Martin Philip Bendsøe and Noboru Kikuchi. Generating optimal topologies in structural design using a homogenization method. *Computer Methods in Applied Mechanics and Engineering*, 71(2):197–224, 1988.

[8] Martin Philip Bendsøe. Optimal shape design as a material distribution problem. *Structural Optimization*, (1):193–202, 1989.

[9] B. Hassani and E. Hinton. A review of homogenization and topology optimization II - analytical and numerical solution of homogenization equations. *Computers & Structures*, 69(6):719–738, 1998.

[10] A. Kaveh, B. Hassani, S. Shojaee, and S.M. Tvakkoli. Structural topology optimization using ant colony methodology. *Engineering Structures*, 2008.

[11] Guan-Chun Luh and Chun-Yi Lin. Structural topology optimization using ant colonu optimization algorithm. *Applied Soft Computing*, 9(4):1343–1353, 2009.

[12] Christian Spada. Aeroelastic Analysis of Nonlinear High Aspect Ratio Wing. Master's thesis, Instituto Superior Técnico, October 2014.